

## A Theoretical Study on the Photoionization of the Valence Orbitals of Phosphine

Edmar M. Nascimento,<sup>a</sup> Luiz E. Machado,<sup>\*,b</sup> Evandro M.S. Ribeiro,<sup>c</sup> Luiz M. Brescansin<sup>d</sup>  
and Mu-Tao Lee<sup>e</sup>

<sup>a</sup>Instituto de Física, Universidade Federal da Bahia, 40210-340 Salvador-BA, Brazil

<sup>b</sup>Departamento de Física and <sup>e</sup>Departamento de Química, Universidade Federal de São Carlos,  
13565-905 São Carlos-SP, Brazil

<sup>c</sup>Instituto de Física de São Carlos, Universidade de São Paulo, CP 369 13560-970 São Carlos-SP, Brazil

<sup>d</sup>Instituto de Física "Gleb Wataghin", Universidade Estadual de Campinas, 13083-970 Campinas-SP, Brazil

Apresentamos um trabalho teórico sobre a fotoionização da fosfina ao nível estático-troca e da aproximação de caroço congelado, usando o método de frações continuadas. O objetivo principal do presente estudo é investigar até que ponto a descrição Hartree-Fock do alvo é válida, quando aplicada em estudos de fotoionização molecular. Também analisamos o papel desempenhado pelos acoplamentos multicanais. Nosso estudo mostra que cálculos Hartree-Fock monocanais podem fornecer resultados confiáveis, exceto para energias do fóton próximas ao limiar da fotoionização.

We report a theoretical study on the photoionization of phosphine in the static-exchange level and frozen core approximation, using the method of continued fractions. The main subject of the present study is to investigate in which extent the Hartree-Fock description of the target applied to molecular photoionization is valid. Also, the role played by multichannel coupling is analysed. Our study shows that single-channel Hartree-Fock calculations can provide reliable results except for photon energies near the photoionization threshold.

**Keywords:** photoionization cross section, photoionization asymmetry parameters, MCF, PH<sub>3</sub>, phosphine

### Introduction

Phosphine is a colorless, flammable, and toxic gas. This compound has important applications in several fields. For instance, in semiconductor technology, phosphine is used in silicon processing as a source for phosphorous implantation.<sup>1</sup> Also in agriculture, it has been widely used as a pesticide.<sup>2,3</sup> Particularly, for the latter application, photodecomposition is a very important mechanism for pesticide degradation and therefore studies on photoionization of this chemical species can contribute to environmental protection. Despite that, both experimental and/or theoretical studies on photoionization of phosphine are very limited. To our knowledge, there is only one experimental measurement of photoabsorption and photoionization cross sections for this molecule reported by Zarate *et al.*<sup>4</sup> Experimental measurements of asymmetry

parameters for photoionization from the valence orbitals of this molecule have been reported by Cauletti *et al.*<sup>5</sup> Theoretically, one of the pioneer studies on photoionization of PH<sub>3</sub> was performed in 1998 by Stener and Decleva<sup>6</sup> using a B-spline calculation based on the density functional theory (DFT) approach. Lately, these authors have improved their method by using a time-dependent density functional theory (TD-DFT) approach<sup>7,8</sup> in which an explicit treatment of the unbound continuum wave function and a linear response of the system to the external weak electromagnetic field are considered. Also, an *ab initio* study using a combination of the K-matrix (KM) technique and the random-phase approximation (RPA) was performed by Carravetta and Cacelli.<sup>9</sup> In this latter study, the KM-RPA method is used as a tool to solve a configuration interaction problem in the continuum through the resolution of the RPA equations, projected on an L<sup>2</sup> basis set, by the K-matrix employed. Therefore these methods account, in some extent, for the electron

\* e-mail: dlem@df.ufscar.br

correlation effects which may be important in molecular photoionization calculations. In addition, the KM-RPA can also describe the coupling of different ionization channels that can be opened in a range of a few eV.

Recently, we have developed a computational code for molecular photoionization calculations based on the method of continued fractions (MCF).<sup>10</sup> In our method, both the ground- and the continuum-state wave functions are described by the Hartree-Fock (HF) approximation. As a first application, the HF-MCF was applied to study the photoionization of the outer-valence orbitals of ammonia.<sup>10</sup> The comparison of our calculated cross sections and asymmetry parameters with the existent theoretical and experimental results was very encouraging. In the present work, we apply the HF-MCF to study the photoionization of the outer-valence orbitals of phosphine at the static-exchange level and frozen core approximation. The comparison of our calculated data with the experimental results can provide information on which extent the HF description of the target applied to molecular photoionization studies is valid. Also, the comparison with the calculated data obtained using a more elaborate theory would provide an insight on the role played by the multichannel-coupling and electron-correlation effects, which can be helpful for improving our method.

## Theory and Calculations

Details of the MCF have been given elsewhere<sup>10-14</sup> so only the essential aspects of the theory will be discussed here. The photoelectron differential cross sections averaged over molecular orientations are given by:

$$\frac{d\sigma^{(L,V)}}{d\Omega_{\vec{k}}} = \frac{\sigma^{(L,V)}}{4\pi} [1 + \beta_k^{(L,V)} P_2(\cos \theta)], \quad (1)$$

where  $\sigma^{(L,V)}$  is the total photoionization cross section, obtained with the length ( $L$ ) or velocity ( $V$ ) form of the dipole moment operator. For nonlinear molecules,  $\sigma^{(L,V)}$  is given by:

$$\sigma^{L,V} = \frac{4\pi E}{3c} \sum_{lm\mu} |I_{lm\mu}^{L,V}|^2 \quad (2)$$

The asymmetry parameter  $\beta_k^{(L,V)}$  appearing in equation (1) can be written as:

$$\beta_k^{L,V} = \frac{3}{5} \left[ \sum_{lm\mu} |I_{lm\mu}^{L,V}|^2 \right]^{-1} (1,1,0,0|2,0) \sum_{lm\mu} \sum_{l'm'\mu'} (I_{lm\mu}^{L,V})^* I_{l'm'\mu'}^{L,V} \quad (3)$$

$$(-1)^{-m'-\mu} [(2l+1)(2l'+1)]^{1/2} (1,1,\mu',-\mu | 2,-M)$$

$$(l,l',0,0 | 2,0)(l,l',m,-m' | 2,M).$$

The quantity  $E$  in equation (2) is the incident photon energy, whereas  $I_{lm\mu}^{L,V}$  in equations (2) and (3) are the partial-

wave components of the dynamical coefficients,  $I_{\vec{k},\hat{n}}^{(L,V)}$

$$I_{\vec{k},\hat{n}}^{(L,V)} = \left( \frac{4\pi}{3} \right)^{\frac{1}{2}} \sum_{lm\mu} I_{lm\mu}^{L,V} Y_{lm}(\hat{k}) Y_{1\mu}(\hat{n}), \quad (4)$$

where

$$I_{\vec{k},\hat{n}}^{(L)} = (k)^{1/2} \langle \Phi_i | \vec{r} \cdot \hat{n} | \Phi_k^{(-)} \rangle \quad (5)$$

and

$$I_{\vec{k},\hat{n}}^{(V)} = \frac{(k)^{1/2}}{E} \langle \Phi_i | \vec{\nabla} \cdot \hat{n} | \Phi_k^{(-)} \rangle. \quad (6)$$

In equations (5) and (6)  $\Phi_i$  is the target ground state wave function,  $\Phi_k^{(-)}$  the final state (incoming-wave normalized) wave function of the system (ion plus photoelectron),  $\hat{n}$  represents the unit vector in the direction of polarization of the radiation and  $\vec{k}$  is the photoelectron momentum.

In the present study,  $\Phi_i$  is an one-determinant wave function calculated at the Hartree-Fock level. The final molecular state is described by a single electronic configuration in which the ionic orbitals are constrained to be identical to those of the initial ground state. In this approximation, the photoelectron orbital  $\Psi_{\vec{k}}^{\pm}(\vec{r})$  is a solution of the one-electron Schrödinger equation

$$\left[ -\frac{1}{2} \nabla^2 + V_{N-1}(\vec{r}; \vec{R}) + \frac{k^2}{2} \right] \Psi_{\vec{k}}^{\pm}(\vec{r}) = 0, \quad (7)$$

where  $\Psi_{\vec{k}}^{\pm}(\vec{r})$  satisfies the appropriate boundary conditions and  $V_{N-1}$  is the static-exchange (SE) potential of the molecular ion with the long-range Coulomb potential of the ionic core removed.<sup>10</sup>

To proceed, equation (7) is rewritten in an integral form, the Lippmann-Schwinger equation, as follows:

$$|\Psi_{\vec{k}}^p\rangle = |u_0^p\rangle + G_c^p U^{(0)} |\Psi_{\vec{k}}^p\rangle \quad (8)$$

and then is solved using the MCF. In equation (8)  $\Psi_{\vec{k}}^p$  is the state vector corresponding to the principal-value of the photoelectron wave function,  $G_c^p$  is the principal value coulombic Green's operator,  $u_0^p$  is a state vector corresponding to the principal value of the coulombic wave function and  $U^{(0)} = 2V_{N-1}$  is the reduced potential operator. Accordingly, the reactance  $\mathbf{K}$  matrix is given by

$$\mathbf{K} = -k \langle u_0 | U^{(0)} | \Psi_{\vec{k}}^p \rangle. \quad (9)$$

The MCF projects the interaction potential on a finite set of functions generated at each step of an iterative procedure and requires no basis functions for the solution of the continuum wave function. So we define the  $n$ th-

order weakened potential operator  $U^{(n)}$  as

$$U^{(n)} = U^{(n-1)} - U^{(n-1)} |u_{n-1}\rangle \mathbf{D}_{2n-1}^{-1} \langle u_{n-1}| U^{(n-1)}. \quad (10)$$

Therefore, the reactance  $\mathbf{K}$  matrix results in the form of a continued fraction. The  $n^{\text{th}}$ -order correction of the matrix is given by

$$\mathbf{K}_n = \mathbf{D}_{2n} + \mathbf{D}_{2n+1} [\mathbf{D}_{2n+1} - \mathbf{K}_{n+1}]^{-1} \mathbf{D}_{2n+1}, \quad (11)$$

where

$$\mathbf{D}_{2n} = \langle u_{n-1} | U^{(n-1)} | u_n \rangle \quad (12)$$

$$\mathbf{D}_{2n+1} = \langle u_n | U^{(n)} | u_n \rangle \quad (13)$$

and

$$|u_n\rangle = G_c^p U^{(n-1)} |u_{n-1}\rangle. \quad (14)$$

The reactance matrix is given by

$$\mathbf{K} = -k\mathbf{D}, \quad (15)$$

where

$$\mathbf{D} = \mathbf{D}_1 + \mathbf{K}_1 [\mathbf{D}_1 - \mathbf{K}_1]^{-1} \mathbf{D}_1, \quad (16)$$

with

$$\mathbf{K}_1 = \langle u_o | U^{(0)} | \Psi_1 \rangle \quad (17)$$

and

$$|\Psi_1\rangle = |u_n\rangle + |\Psi_{n+1}\rangle [\mathbf{D}_{2n+1} - \mathbf{K}_{n+1}]^{-1} \mathbf{D}_{2n+1}. \quad (18)$$

It is expected the operator  $U^{(n)}$  to become weaker and weaker with increasing  $n$ . As a result, the iterative procedure can be stopped after some number of steps, when the desired convergence is achieved. The converged  $\mathbf{K}$  matrix corresponds to the exact solution for a given potential  $U^{(0)}$  in equation (8).  $\mathbf{K}_1$  can be obtained backwardly using equation (11) by setting  $\mathbf{K}_{n+1} = 0$ . Then, the  $\mathbf{D}$  matrix is obtained using equation (16). In order to constrain the continuum solution to be orthogonal to the occupied bound orbital ( $\phi_i$ ), the short-range portion of the static-exchange potential is calculated using a generalized Phillips-Kleinman pseudopotential defined by<sup>15</sup>

$$V_{orth} = V_{SE} - LQ - QL + QLQ \quad (19)$$

where  $V_{SE}$  is the usual static-exchange potential and

$$L = -\frac{1}{2} \nabla^2 - \varepsilon + V_{SE} \quad (20)$$

$$Q = \sum_{i=1}^n |\phi_i\rangle \langle \phi_i|. \quad (21)$$

In equation (20)  $\varepsilon$  is the photoelectron energy.

## Results and Discussion

The ground state of neutral  $\text{PH}_3$  belongs to  $C_{3v}$  symmetry and has the electronic configuration

**Table 1.** Gaussian basis sets for the ground state of the  $\text{PH}_3$  molecule

	s		p		d	
Center	Exp.	Coef.	Exp.	Coef.	Exp.	Coef.
P	77492.4300	0.000787	384.8400	0.003240	1.6000	1.000000
	11605.7900	0.006107	90.5520	0.024925	0.4000	1.000000
	2645.9600	0.031373	28.8060	0.105697		
	754.9800	0.124239	10.6880	0.263229		
	248.7500	0.380893	4.2521	0.719052		
	91.1570	0.559811	4.2521	-1.612718		
	91.1570	0.163986	1.7405	1.205067		
	36.2260	0.625951	0.5979	1.000000		
	15.2110	0.262196	0.2292	1.000000		
	4.7138	1.000000	0.0838	1.000000		
	1.7827	1.000000				
	0.3425	1.000000				
	0.1246	1.000000				
	H	33.6400	0.025374			
5.0580		0.189681				
1.1470		0.852921				
0.3211		1.000000				
0.1013		1.000000				

$$(1a_1^2 2a_1^2 1e^4 3a_1^3)(4a_1^2 2e^4 5a_1^2): {}^1A_1. \quad (22)$$

The corresponding SCF-HF wavefunction was obtained using the basis set shown in Table 1. At the equilibrium geometry ( $r_{\text{PH}} = 1.42 \text{ \AA}$  and  $\text{PHP} = 93.3454^\circ$ , Ref. 9) this basis set gives an SCF energy of  $-342.46998$  a.u., which can be compared with the SCF energy of  $-342.36424$  a.u. of Carravetta and Cacelli<sup>9</sup> and with the RHF value of  $-342.4934$  of Clark *et al.*<sup>16</sup> Our calculated dipole moment was  $0.541$  D, to be compared with the calculated value of  $0.624$  D of Clark *et al.*<sup>16</sup> and with the experimental value of  $0.578$  D of Burrus.<sup>17</sup> The static potential was evaluated using a single-center expansion truncated at  $l_{\text{max}} = 20$ , and all matrix elements arising in the MCF were calculated with  $l_{\text{max}} = 6$ , retaining all allowed  $|m| \leq 1$  for a given  $l$ . In all of our calculations convergence was achieved within five iterations.

Firstly, we intend to compare the results of our calculations at the Hartree-Fock (HF) and single-channel (SC) level with the available experimental results as well as with other reported calculations at the same SC level. Figures 1(a) and 2(a) show our calculated results of  $\sigma$  for the photoionization out of the two outermost orbitals  $5a_1$  (IP =  $10.6$  eV) and  $2e$  (IP =  $13.6$  eV), respectively. The results are presented in both dipole-length (DL) and dipole-velocity (DV) forms, along with theoretical DL results obtained by Stener and Decleva<sup>6</sup> using the B-spline technique and with those obtained by Carravetta and Cacelli<sup>9</sup> using the SC-RPA. The experimental results of Zarate *et al.*<sup>4</sup> are also included for comparison. The observed differences between our DL and DV results can be attributed to the neglect of the electronic correlation in the target wavefunction.<sup>9,18</sup> Our HF-SC results do not reproduce the sharp fall-off of  $\sigma$  near the threshold seen in both the experimental and SC-RPA data. Probably, this is also due to that neglect. Away from this region, it is observed that the experimental results for  $\sigma$  lay between our DL and DV results, in such a way that for the  $5a_1^{-1}$  channel our DL results agree better with the experimental data, whereas for the  $2e^{-1}$  channel our DV results do so. The DL results of the B-spline DFT calculation of Stener and Decleva<sup>6</sup> lay well below the experimental results for both channels.

Comparison of our HF-SC theoretical results for  $\beta$  with experimental results of Cauletti *et al.*<sup>5</sup> and with the theoretical<sup>6,9</sup> data is shown in the Figures 1(b) and 2(b), for photoionization out of the  $5a_1$  and  $2e$  orbitals, respectively. Both our DL and DV results are in reasonable good agreement with the experimental results<sup>5</sup> and with the SC-RPA data of Carravetta and Cacelli<sup>9</sup> in the entire energy range, whereas the B-spline DFT results of Stener and Decleva<sup>6</sup> underestimate the experimental data in the low-energy region, for both

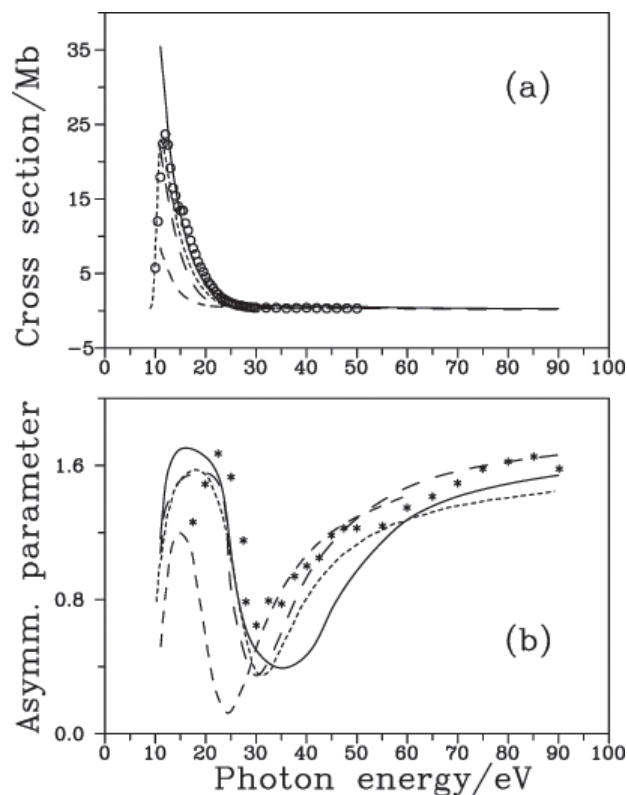


**Figure 1.** (a) Cross sections and (b) asymmetry parameters for photoionization leading to the  ${}^2A_1(5a_1^{-1})$  state of  $\text{PH}_3^+$ . Solid line, present DL results; long-dashed line, present DV results; dashed line, DL results of Stener and Decleva<sup>6</sup> using the B-spline technique and with those obtained by Carravetta and Cacelli<sup>9</sup> using the SC-RPA. The experimental results of Zarate *et al.*<sup>4</sup> are also included for comparison. The observed differences between our DL and DV results can be attributed to the neglect of the electronic correlation in the target wavefunction.<sup>9,18</sup> Our HF-SC results do not reproduce the sharp fall-off of  $\sigma$  near the threshold seen in both the experimental and SC-RPA data. Probably, this is also due to that neglect. Away from this region, it is observed that the experimental results for  $\sigma$  lay between our DL and DV results, in such a way that for the  $5a_1^{-1}$  channel our DL results agree better with the experimental data, whereas for the  $2e^{-1}$  channel our DV results do so. The DL results of the B-spline DFT calculation of Stener and Decleva<sup>6</sup> lay well below the experimental results for both channels.

channels. Also, the positions of the maximum and minimum structures are generally well reproduced by our results, whereas the DL results of Stener and Decleva<sup>6</sup> show minima that are shifted to lower energies, mainly for the photoionization out of the  $2e$  orbital.

In order to estimate the effects of multi-channel (MC) coupling, in Figures 3 and 4 we compare our DL results for the  $5a_1$  and  $2e$  channels, respectively, with the corresponding MC-RPA results of Carravetta and Cacelli<sup>9</sup>, as well as with the experimental results of Zarate *et al.*<sup>4</sup> and Cauletti *et al.*<sup>5</sup> The calculated DL data using the TD-DFT approach<sup>7,8</sup> are also shown in these figures for comparison. For both  $\sigma$  and  $\beta$  quantities, our results for energies above  $12$  eV (for  $5a_1^{-1}$ ) and  $15$  eV (for  $2e^{-1}$ ) reproduce fairly well the multi-channel results of Carravetta and Cacelli.<sup>9</sup> On the other hand, at lower energies, the MC-RPA  $\sigma$  results of Carravetta and Cacelli also show the correct near-threshold behavior, thus confirming that such a behavior can only be described by the inclusion of the electronic correlation effects in the target wavefunction.<sup>9</sup> In contrast, the MC and the SC results of Carravetta and Cacelli<sup>9</sup> for  $\beta$  are not

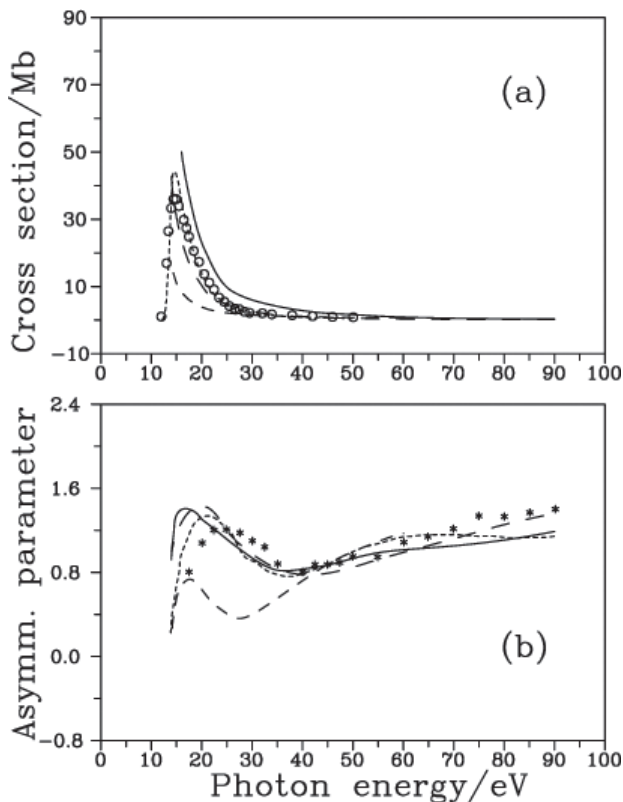


Figure 2. Same as in Figure 1 but for the  ${}^2E(2e^{-1})$  state of  $\text{PH}_3^+$ .

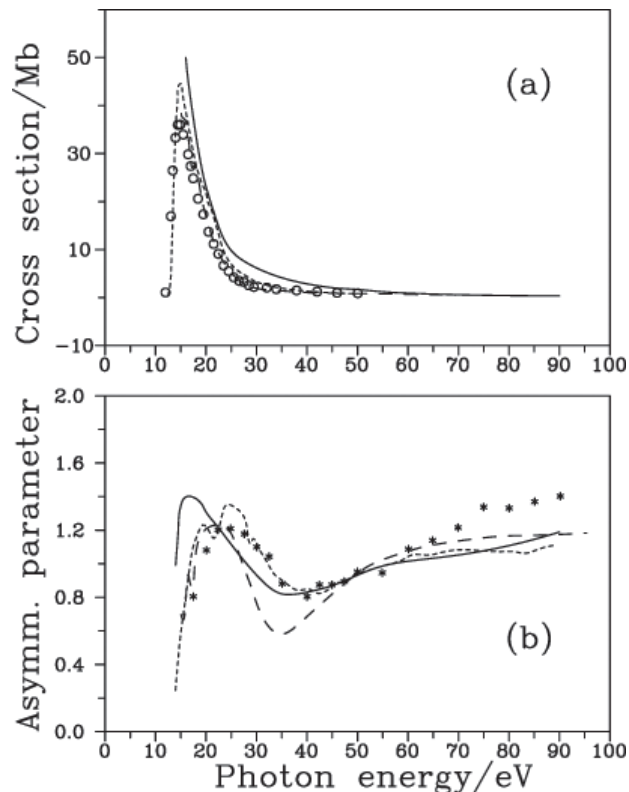


Figure 4. Same as in Figure 3 but for the  ${}^2E(2e^{-1})$  state of  $\text{PH}_3^+$ .

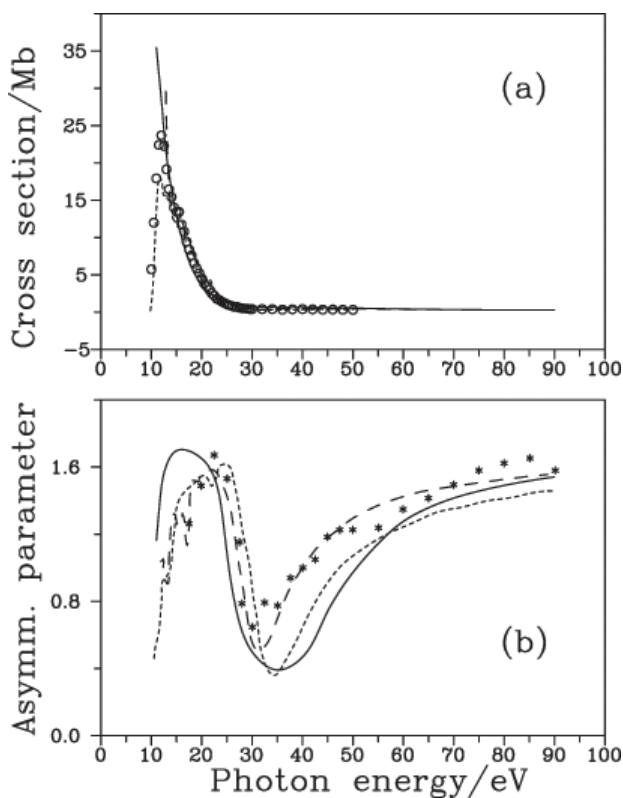


Figure 3. Same as in Figure 1. Solid line, present DL results; short-dashed line, MC-RPA DL results of Carravetta and Cacelli (from ref. 9); dashed line, TD-DFT DL results of Fronzoni *et al.* (from ref. 8); open circles, experimental results of Zarate *et al.* (from ref. 4); asterisks, experimental results of Cauletti *et al.* (from ref. 5).

substantially different, except for the occurrence of some structures that are seen in the MC results which can be attributed to the inter-channel coupling. In addition, the deficiency observed in the Kohn-Sham DFT results, seen in Figures 1 and 2, is completely recovered by the TD-DFT approach<sup>7,8</sup> in such a way that the TD-DFT results for both  $\sigma$  and  $\beta$  agree much better with the experimental data<sup>4</sup> and with the RPA results of Carravetta and Cacelli<sup>9</sup>. The response of the system to the external time-varying field has been attributed by the authors<sup>7,8</sup> as the physical origin of this improvement. This statement, however, may not be true since our HF-SC results, although not accounting for such a response, are already in good agreement with both the TD-DFT and the experimental results. Therefore, we believe that the explicit treatment of the unbound continuum wave function may be responsible for that improvement. Moreover, the structures seen in the TD-DFT results for both  $\sigma$  and  $\beta$ , due to the occurrence of Feshbach one-electron autoionization resonances, suggest that the TD-DFT calculations are of multichannel nature.

In summary, we have shown that our HF-SC calculation can provide reliable results for both  $\sigma$  and  $\beta$  in the energy range from a few eV above threshold to intermediate energies. However, the near-threshold fall-off of the  $\sigma$  values can only be well described in the framework of

approximations beyond the HF level. On the other hand, both  $\sigma$  and  $\beta$  are only slightly influenced by a multi-channel treatment. Considering the numerical simplicity of our method, it can be considered an adequate tool for the treatment of valence-shell molecular photoionization, specially for heavier molecules. A more complete treatment for such systems would constitute a formidable computational task.

## References

1. Adler, J.; Doering, H.R.; Grosse, H.J.; Gleisberg, F.; *Zfl. Mitt.* **1983**, *69*, 328.
2. Scudamore, K.A.; Goodship, G.; *Pestic. Sci.* **1986**, *17*, 385
3. Leitao, J.; De Saint Blanquat, G.; Bailly, J.R.; *Appl. Environ. Microbiol.* **1987**, *53*, 2328.
4. Zarate, E.B.; Cooper, G.; Brion, C.E.; *Chem. Phys.* **1990**, *148*, 277.
5. Cauletti, C.; Adam, M.Y.; Piancastelli, M.N.; *J. Electron Spectrosc. Relat. Phenom.* **1989**, *48*, 379.
6. Stener, M.; Decleva, P.; *J. Electron Spectrosc. Relat. Phenom.* **1998**, *94*, 195.
7. Stener, M.; Decleva, P.; *J. Chem. Phys.* **2000**, *112*, 10871.
8. Fronzoni, G.; Stener, M.; Decleva, P.; *J. Chem. Phys.* **2003**, *118*, 10051.
9. Carravetta, V.; Cacelli, I.; *Chem. Phys.* **1999**, *243*, 77.
10. Nascimento, E.M.; Ribeiro, E.M.S.; Brescansin, L.M.; Lee, M.-T.; Machado, L.E.; *J. Phys. B* **2003**, *36*, 3621.
11. Horacek, J.; Sasakawa, T.; *Phys. Rev. A* **1983**, *28*, 2151.
12. Horacek, J.; Sasakawa, T.; *Phys. Rev. A* **1984**, *30*, 2274.
13. Lee, M.-T.; Iga, I.; Fujimoto, M.M.; Lara, O.; *J. Phys. B* **1995**, *28*, L299.
14. Ribeiro, E.M.S.; Machado, L.E.; Lee, M.-T.; Brescansin, L.M.; *Comp. Phys. Comm.* **2001**, *136*, 117.
15. Lucchese, R.R.; Raseev, G.; McKoy, V.; *Phys. Rev. A* **1982**, *25*, 2572.
16. Clark, S.A.C.; Brion, C.E.; Davidson, E.R.; Boyle, C.; *Chem. Phys.* **1989**, *136*, 55.
17. Burrus, C.A.; *J. Chem. Phys.* **1958**, *28*, 427.
18. Cacelli, I.; Moccia, R.; Montuoro, R.; *Phys. Rev. A* **2000**, *63*, 012512.

Received: March 24, 2005

Published on the web: January 13, 2006

FAPESP helped in meeting the publication costs of this article.